



XA0054025

CRYOGENIC DEUTERIUM Z-PINCH AND WIRE ARRAY Z-PINCH STUDIES AT IMPERIAL COLLEGE.

M.G. Haines, R. Aliaga-Rossel, F.N. Beg, A.R. Bell, S. Channon, J.P. Chittenden, M. Coppins, A.E. Dangor, D.F. Howell, N.G. Kassapakis, S.V. Lebedev, I.H. Mitchell, J. Ruiz-Camacho, J.F. Worley & D. Zdravkovic

The Blackett Laboratory, Imperial College, London SW7 2BZ, U. K.

I. Ross

A.W.E. Aldermaston, Reading, RG7 4PR, U. K.

Abstract

Z-pinch experiments using cryogenic deuterium fibre loads have been carried out on the MAGPIE generator at currents up to 1.4MA. $M=0$ instabilities in the corona caused plasma expansion and disruption before the plasma could enter the collisionless Large ion Larmor radius regime. For the last 12 months we have studied Aluminium wire array implosions using laser probing, optical streaks and gated X-ray images. Plasma from the wires is accelerated to the axis as radial plasma streams with uncorrelated $m=0$ instabilities superimposed. Later in the discharge a global Rayleigh-Taylor (R-T) instability develops. Single and double aluminium and tungsten wire shots were conducted at 150kA. 2-D and 3-D simulations and a heuristic model of wire arrays will be presented along with theories on the combined MHD/R-T instability and sheared axial flow generation by large ion Larmor radius effects.

1. CRYOGENIC DEUTERIUM FIBRE Z-PINCHES

The MAGPIE generator (2.4MV, 1.9MA) was employed to discharge currents of up to 1.4MA through cryogenic deuterium fibres of 100 μ m diameter and 23 mm in length with a current rise time of 150ns. Optical and X-ray streak and framing cameras and laser interferometry and schlieren were employed, and gave results similar to those found in our earlier experiments with carbon and CD₂ fibres, the parameters of the coronal plasma being practically independent of the material and initial fibre diameter. In all experiments, the corona plasma was observed (in laser schlieren images) to expand at a constant $5 \times 10^4 \text{ ms}^{-1}$ and to be susceptible to $m=0$ instabilities right from the very start of the discharge (see Figure 1). The measured expansion velocity of the plasma and the observed evolution of the characteristic 1mm wavelength for the $m=0$ instability are in close agreement with the results of 2-D resistive MHD simulations of carbon fibres [1], which also indicated insensitivity of the coronal behaviour to the initial fibre diameter.

In experiments using D₂ fibre loads, bursts of 10^8 - 10^9 neutrons occurred late in the discharge as a result of ion acceleration processes in the rarefied plasma gaps which result from the substantial $m = 0$ instability activity. Discharges into low line density, 7 μ m diameter carbon fibres do not show improved stability of the coronal plasma. Moreover, disruption of the discharge (transition to the e-beam generation mode) occurs earlier than for thicker fibres and before sufficient current is reached for the ions to become collisionless and for pinch to enter the large Larmor radius (LLR) regime [2].

A current pre-pulse of 30kA was found to convert 1% of the fibre mass into a low density corona

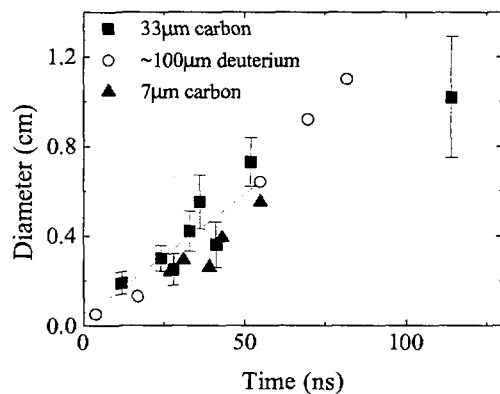


Figure 1a. Coronal plasma diameter versus time for various fibres.

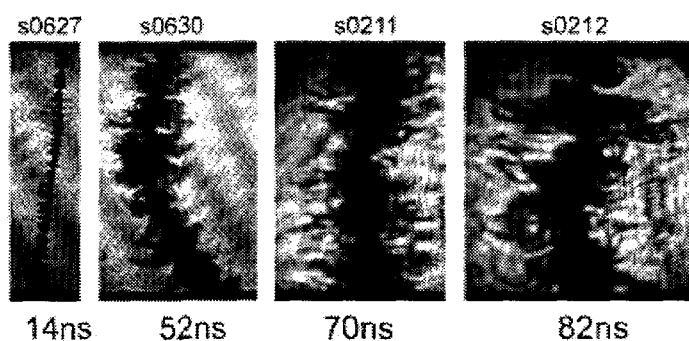


Figure 1b. Schlieren photographs from different discharges into 100 μ m deuterium fibres

around the fibre. This reduced both the $m=0$ instability development and the radial expansion velocity during the initial phase of the discharge compared to shots with no pre-pulse. It is possible that a more controllable and effective pre-ionisation of the fibre would allow further improvements to the stability of a z-pinch initiated from a solid fibre.

2. WIRE ARRAY Z-PINCH EXPERIMENTS

Wire arrays 16 mm in diameter and 23 mm long with 8 to 64 aluminium wires of 15 μm diameter were imploded on the MAGPIE generator, stagnating on axis near the current maximum (1.4 MA at 240 ns) to form a hot dense plasma. Both end-on ($r-\theta$ plane) and side-on ($r-z$ plane) laser probing (Nd-YAG, 532 nm, 0.4 ns) was used giving interferometry, schlieren or shadow images. A gated 4-frame camera (2 ns gating time, 9 ns separation) gave time-resolved soft X-ray images.

End-on ($r-\theta$ plane) interferograms (Fig 2) show that after 60ns, the plasma from the wires starts to move inside the array in the form of radially directed streams. The plasma electron density contour of 10^{23} m^{-3} has an inward radial velocity of $\sim 1.5 \times 10^5 \text{ ms}^{-1}$ while the azimuthal velocity is 1/4 of the radial velocity. Azimuthal expansion leads to merging of the coronal plasmas and plasma with density $> 10^{23} \text{ m}^{-3}$ fills the regions between the wires at the initial radius of the array at 65 and 90 ns for arrays with 64 and 8 wires (gap size 0.78-6.28 mm) respectively.

Side-on laser probing (at a higher electron density of 10^{25} m^{-3}) shows the same 60 ns delay before rapid expansion at $3.2 \times 10^4 \pm 3 \times 10^3 \text{ ms}^{-1}$ in the inward radial direction and $1.32 \times 10^4 \pm 1 \times 10^3 \text{ ms}^{-1}$ in the azimuthal direction. This expansion occurs with the development of $m=0$ like instabilities with axial wavelength less than 0.5 mm. The global magnetic field of the array modifies the instability pattern, which is no longer symmetric around each wire axis. Comparison of the instabilities in different wires shows that they are not correlated during the initial stages of the discharge.

Coronal plasma is observed on axis in radial optical streak photographs, x-ray gated images and laser probing (Fig 3) long before the final array implosion where it accumulates forming a precursor pinch of $\sim 1\text{mm}$ diameter. The precursor formation time of ~ 120 ns implies 1keV ions and is relatively insensitive to the number of wires in the array, however, the intensity and diameter of precursor plasma emission in both the optical and x-ray regions decrease as the number of wires increases.

During the later stages of array implosion, the development of a global $m=0$ instability with a dominant wavelength of 1.7-2.3 mm was observed by a number of diagnostics, starting at time $t/t_{\text{imp}} \sim 0.7 - 0.8$ (where t_{imp} is the calculated time of implosion). X-ray gated images show that a number of axially correlated bright spots are formed at the initial radial positions of wires (Figure 4). The same characteristic wavelength of $\sim 2\text{mm}$ of instability is also seen in side-on laser probing images and axial streak photographs, which both show the formation of radially directed plasma streams and axial gaps. The scaling of the time of appearance of the global instability with the number of wires (N) is consistent with a heuristic model [3] for the magnetic Rayleigh-Taylor instability whose initial perturbation amplitude (δ_0) is determined by averaging the initial uncorrelated instabilities on the individual wires and is proportional to $N^{-1/2}$ [4], (see Figure 5).

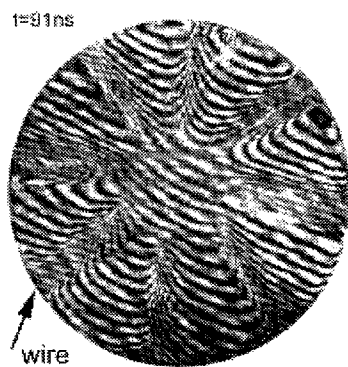


Fig 2. End-on interferogram of an 8 wire array.

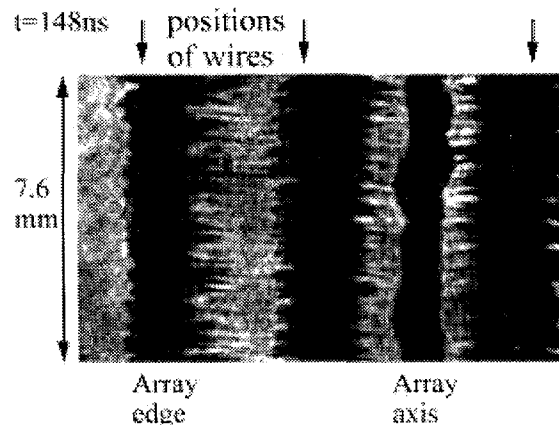


Fig 3. Side-on Schlieren of an 8 wire array, showing coronal plasma around the wires and the precursor on axis.

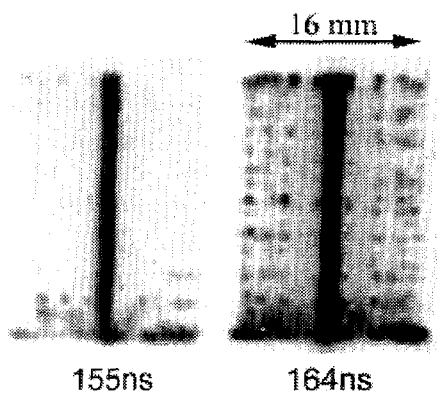


Figure 4. Gated soft X-ray images of hot-spot formation on 16 wires in an array.

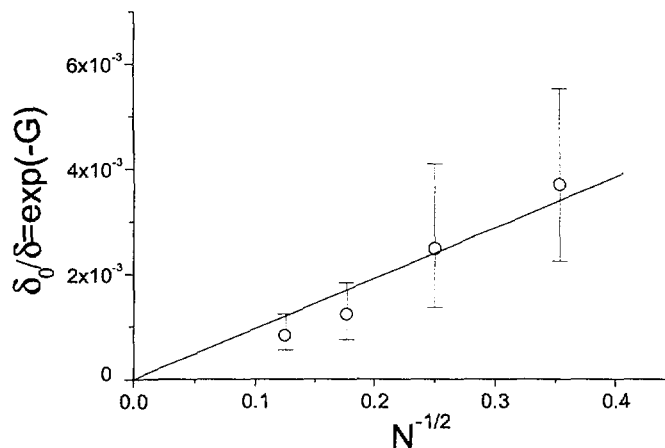


Figure 5. Fit of the experimentally implied global perturbation amplitude to data to $N^{-1/2}$.

3. WIRE ARRAY Z-PINCH SIMULATIONS

We have developed a three dimensional resistive MHD code for the simulation of wire arrays. The model is two temperature (electrons and ions) and incorporates LTE ionisation dynamics and a simple radiation loss model. Explicit hydrodynamics is performed on a Cartesian (x,y,z) Eulerian grid, using second order Van-Leer advection. The thermal and magnetic field diffusion equations are solved implicitly using an iterative matrix inversion method.

A 2D (r,z) resistive MHD code (with fine spatial resolution) is used to model the initial ablation phase of the wires and provide the starting conditions for 3D code runs on a coarser grid. Cold-start conditions are applied in the 2D(r,z) code with a Thomas-Fermi equation of state and transport coefficients which model the transition from solid to plasma conductivity. Fig 6 shows a mass density map from a 2D(r,z) simulation of a $15\mu\text{m}$ aluminium wire carrying an eighth of the total MAGPIE current. Despite being surrounded by a high temperature corona exhibiting an $m=0$ instability with 0.5 mm wavelength, the cold unionised core of the wire still retains 83% of the original mass. Three-dimensional results show that the symmetry of implosion is strongly affected by the level of ionisation provided by the 2-D code.

Computational resources presently limit high resolution results from the 3-D code to 2D in the x-y plane. Fig 7 shows a logarithmic mass density contour map of one quarter of an array of 8 $15\mu\text{m}$ aluminium wires driven by MAGPIE. Low density coronal material is swept around the higher density wire cores by the global magnetic field giving rise to radial streams of plasma and forming a precursor on axis. Fig 8 shows one iso-density contour at 170ns from a low resolution 3D simulation of the same experiment. An imposed perturbation on the wires has resulted in plasma in some axial positions being pinched to the axis (the back-right corner) before plasma in adjacent regions has begun to move.

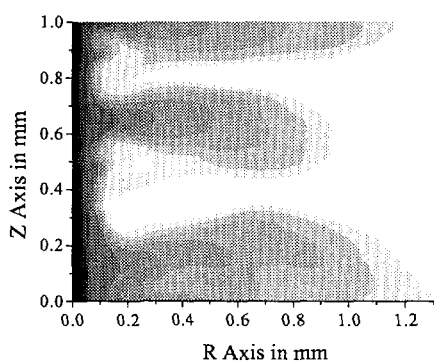


Fig 6. $\rho(r,z)$ from a cold start simulation of an Al wire, at 100ns.

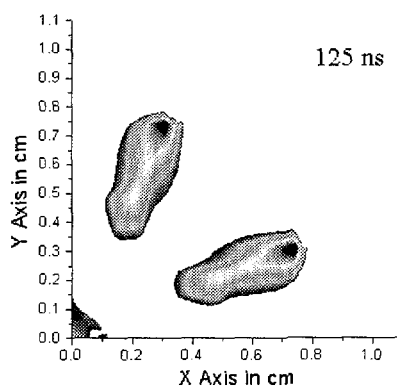


Fig 7. $\rho(x,y)$ from a simulation of a 8 wire Al array, at 125ns.

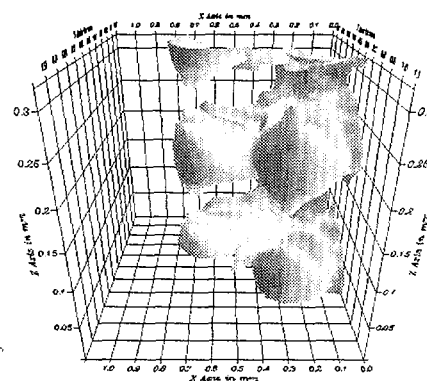


Fig 8. $\rho(x,y,z)$ contour at 170ns from a 3D array simulation of 8 wires Al.

4. THEORETICAL MODELS OF Z-PINCHES

A heuristic model of the wire array pinch divides the dynamics into four phases. In the first, each wire is transformed into an expanding plasma with uncorrelated MHD instabilities as in single wire experiments. The global magnetic field causes radial elongation of the plasma emanating from the wires and determines the shell thickness when these plasmas merge (the second phase). The global perturbation amplitude is then $N^{-1/2}$ times the amplitude of the uncorrelated instabilities in the individual wires. Phase 3 is the inward acceleration of the shell, with the linear and non-linear evolution of the Rayleigh-Taylor instability. At phase 4, the stagnation, the amplitude of the dominant R-T mode, the shell thickness and the final implosion velocity determine the X-ray pulse. The energy, at first in the ions, is randomised and equipartition to the electrons leads to rapid ionisation and radiation loss. For low N implosions in Al, the equipartition time is much longer than the Alfvén transit time and this leads to a broadening of the X-ray pulse. Good agreement with Sandia experiments is found.

The stability of rapidly imploding uniform-fill gaseous Z-pinches has been studied using a 2D(r,z) MHD code. Unlike hollow cylindrical shell implosions, these pinches do not exhibit classical Rayleigh-Taylor like growth, but rather follow MHD behaviour with the growth rate being inversely proportional to the radius. At peak compression, the instability mode structure at the pinch surface is destroyed by a shock wave reflected from the pinch axis, however, after a recovery time given by the instability scale-length divided by the thermal velocity, the mode structure is re-established.

Investigations of the stabilising effects of sheared axial flow in both the linear and non-linear MHD regimes show that whilst reductions in growth rates are possible, overall stability is not. A Vlasov-fluid model of a Z-pinch in the large Larmor radius regime has been used to demonstrate the spontaneous generation of sheared axial flow caused by the interaction of ions with a moving vacuum / plasma boundary (*Fig. 9*). Optimum shear generation occurs at the same value of Larmor radius (10-15% of pinch radius) as the maximum reduction in the linear growth rate for $m=0$ and $m=1$ modes [5].

5. Z-PINCH EXPERIMENTS WITH ONE OR TWO WIRES.

Experiments at 150kA with single wires show that whilst the expansion velocity of aluminium coronal plasma is typically twice that of tungsten, it is relatively insensitive to the wire diameter. Experiments with two wires separated by 300, 600 and 1500 μm show plasma regions both localised to the wires and equispaced between the wires. The central plasma formation time depends on material and separation, appearing at 5, 15 and 30 ns for aluminium wires separated by 300, 600 & 1500 μm . With 600 μm separation, the instabilities on the wires are correlated after 15ns. The global magnetic field results in faster expansion in the side-on direction than the face-on direction and streams plasma from the wires to the centre. The central plasma increases in size becoming $m=0$ and $m=1$ unstable (*Fig. 10*).

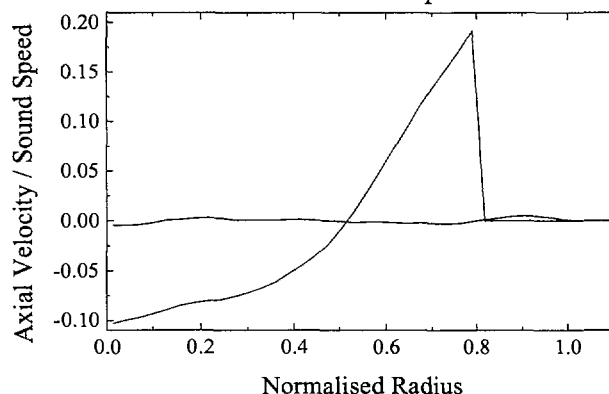


Fig. 9. Axial ion fluid velocity versus radius

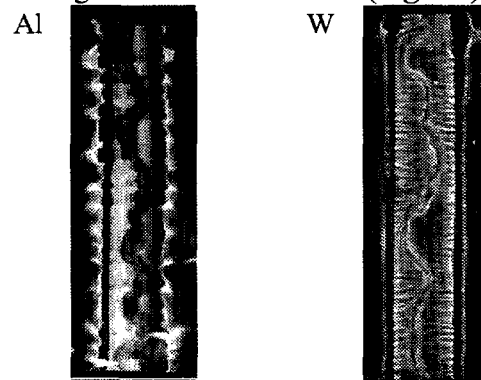


Fig. 10. Schlieren images of 2 wire pinches.

REFERENCES

- 1 J.P. Chittenden, et.al., Phys. Plasmas **4**, 4309 (1997).
- 2 M.G. Haines, M. Coppins, Phys. Rev. Lett. **66**, 1462 (1991).
- 3 M.G. Haines, IEEE Trans. Plasma Science, **26**, 1275 (1998).
- 4 S.V. Lebedev, et.al. (to be published in Phys. Rev. Lett. 1998).
- 5 T.D. Arber, M. Coppins and J. Scheffel, Phys. Rev. Lett, **72**, 2399 (1994)